Matrix Isolation and Ab Initio Study of the Hydrogen-Bonded H_2O_2-CO Complex

Jan Lundell,* Santtu Jolkkonen, Leonid Khriachtchev, Mika Pettersson, and Markku Räsänen[a]

Abstract: The structure, energetics, and infrared spectrum of the H_2O_2-CO complex have been studied computationally with the use of ab initio calculations and experimentally by FTIR matrix isolation techniques. Computations predict two stable conformations for the H_2O_2-CO complex, both of which show almost linear hydrogen bonds between the subunits. The carbon-attached HOOH–CO complex is the lower-energy form, and it has an interaction energy of $-9.0\,kJ\,mol^{-1}$ at the CCSD(T)/6-311++G(3df,3pd)//MP2/6-311++G(3df,3pd) level. The higher-energy form, HOOH–OC, has an interaction energy of $-4.7\,kJ\,mol^{-1}$ at the same level of theory. Experimentally, only the lower-energy form, HOOH–CO, was observed in Ar, Kr, and Xe matrices, and the hydrogen bonding results in substantial perturbations of the observed vibrational modes of both complex subunits. UV photolysis of the complex species primarily produces a complex between water and carbon dioxide, but minor amounts of HCO and *trans*-HOCO were found as well.

Keywords: ab initio calculations · hydrogen bonds · hydrogen peroxide · IR spectroscopy

Introduction

In addition to its industrial uses, hydrogen peroxide (H_2O_2) has an important role in atmospheric chemistry and physics,[1] combustion chemistry[2] and biological processes.[3] Recently, H_2O_2 was found on the surface of Europa, which is one of the satellites of Jupiter.[4] In our atmosphere, hydrogen peroxide serves as a link between gas-phase radicals and aqueous chemistry, and it plays a significant role in the formation of sulfuric acid, the destruction of ozone, and in various oxidation reactions. H_2O_2 is a source of OH radicals in the gas phase upon UV radiation, but the reverse reaction does not normally occur. The only established gas-phase source of tropospheric hydrogen peroxide is the recombination of two HO_2 radicals that form H_2O_2 and O_2,[1] even though there are indirect indications of (OH+OH) recombination in the presence of a third molecule.[5]

Molecular complexes of atmospheric constituents have been noted to affect atmospheric chemistry and physics.[6] The low-frequency intermolecular vibrations have been designated as important channels for the absorption of both solar radiation that enters the atmosphere and the outgoing infrared (IR) surface radiation.[7, 8] Furthermore, atom-molecule complexes, such as $H_2O-O(^3P)$, can contribute to the atmospheric chemistry of hydrogen peroxide, especially since this particular complex has already been shown in laboratory conditions to produce H_2O_2 upon UV irradiation.[9–11] Experimental reports of weakly bound complexes that involve hydrogen peroxide are relatively sparse. Nevertheless, low-temperature solids have been employed to isolate reactive species, and a few studies have addressed complexes of hydrogen peroxide.[12–14] Tso and Lee studied $H_2O_2/H_2O/CO$ mixtures in oxygen matrices[12] and identified some vibrational bands of both H_2O and CO complexes with H_2O_2. The hydrogen peroxide complex with molecular nitrogen was studied by our group[13] in conjunction with our studies of hydrogen peroxide in various rare gas matrices.[9–11, 15] The method for the preparation of monomeric hydrogen peroxide in a low-temperature matrix was devised in our laboratory[15] for these studies, and was also used by Ault and co-workers to study the hydrogen-bonded complex of H_2O_2 and $(CH_3)_2O$ in solid argon.[14]

Due to the importance of the chemistry of H_2O_2 in various fields, a plethora of theoretical studies have been conducted on weak chemical interactions that involve hydrogen peroxide. Hydrogen peroxide forms cyclic dimers,[16–18] which are potential impurities in experimental work. Ab initio studies on H_2O_2 complexes with water,[19, 20] hydrogen halides,[21] and biologically important molecules[22] indicate that hydrogen peroxide is a better proton donor for hydrogen bonding than water.

[a] Dr. J. Lundell, Dr. S. Jolkkonen, Dr. L. Khriachtchev, Dr. M. Pettersson, Prof. M. Räsänen
Laboratory of Physical Chemistry
P.O. Box 55 (A.I.Virtasen aukio 1)
00014 University of Helsinki (Finland)
Fax: (+358) 9-191-50279
E-mail: lundell@csc.fi

0947-6539/01/0708-1670 $ 17.50+.50/0

Table 1. The optimized equilibrium geometries[a] of the HOOH – CO and HOOH – OC complexes.

	HOOH – CO			HOOH – OC		
	MP2/ 6-311++G(2d,2p)	MP2/ 6-311++G(3df,3pd)	MP3/ 6-311++G(2d,2p)	MP2/ 6-311++G(2d,2p)	MP2/ 6-311++G(3df,3pd)	MP3/ 6-311++G(2d,2p)
r(O–H)	0.963	0.962	0.956	0.963	0.963	0.957
r(O–O)	1.459	1.443	1.439	1.458	1.442	1.439
r(O–H_{HB})	0.966	0.966	0.959	0.963	0.962	0.957
r(C≡O)	1.135	1.131	1.119	1.137	1.134	1.122
r(H···C)	2.203	2.172	2.270			
r(H···O)				2.230	2.179	2.240
r(O···C)	3.151	3.119	3.204			
r(O···O)				3.159	3.107	3.175
α(O-O-H)	99.2	99.6	100.8	99.3	99.7	100.7
α(O-O-H_{HB})	99.2	99.6	100.3	99.3	99.7	100.5
α(O-H_{HB}···C)	166.8	166.5	164.5			
α(O-H_{HB}···O)				161.7	161.7	165.7
α(H_{HB}···C≡O)	173.8	173.0	172.5			
α(H_{HB}···O≡C)				170.7	170.7	183.6
α(HOOH)	115.2	112.1	113.2	115.4	112.5	113.1

[a] Bond distances are given in Å and bond angles are in degrees. The HB abbreviation denotes the hydrogen-bonded OH in hydrogen peroxide.

Herein we combine theoretical ab initio calculations and experimental matrix isolation techniques to study the interactions of hydrogen peroxide and carbon monoxide in low-temperature rare gas matrices. We also demonstrate the formation of the H_2O-CO_2 complex as the main photoproduct of the UV-induced reaction of the HOOH – CO complex.

Results and Discussion

Computational results

Equilibrium structures: The potential energy surface (PES) for the H_2O_2 – CO interaction was preliminary scanned at the RHF/6-31+G(d) level of theory. Only two stationary points were found on the PES, both of which involve an almost linear hydrogen bond from the OH group of the hydrogen peroxide molecule to either the oxygen or the carbon terminal of the CO molecule. These stationary points were reoptimized with the use of larger basis sets at the MP2 and MP3 levels, and the bond distances and angles of the equilibrium structures that were obtained are presented in Table 1 (see Figure 1).

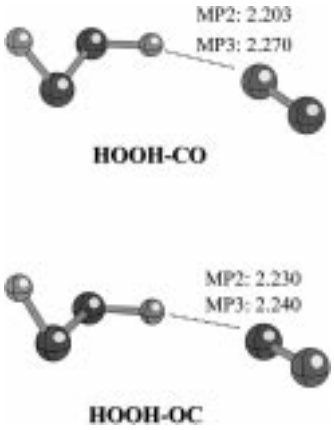

Figure 1. The optimized equilibrium structures of the HOOH···CO and HOOH···OC complexes. The MP2 and MP3 values presented correspond to the intermolecular distance calculated using the 6-311++G(2d,2p) basis set. The numerical parameters are given in Table 1.

The structures of the monomers are perturbed very little upon complexation. For the carbon attached complex HOOH – CO, the hydrogen-bonded O–H bond shows a small elongation of approximately 0.03 Å. The smallest intermolecular (H···C) distance between H_2O_2 and CO is 2.203 Å at the MP2/6-311++G(2d,2p) level. Increasing the basis set by adding polarization functions shortens the bond distance to 2.171 Å, but the effect of increasing the electron correlation has the opposite effect, and at the MP3/6-311++G(2d,2p) level, the (H···C) distance is 2.270 Å. The distance between the heavy atoms O···C range between 3.119 and 3.204 Å, which shows a similar behaviour as the H···O intermolecular distance. For the other complex, HOOH – OC, only nominal effects on the structural properties of the monomers were observed upon complexation. In fact, for the

Abstract in Finnish: *Vetyperoksidin ja hiilimonoksidin muodostamien kompleksien rakenteita, energetiikkaa ja värähdysspektrejä tutkittiin kvanttikemiallisilla laskuilla ja kokeellisella FTIR-matriisi-isolaatiotekniikalla. Laskennallisesti löysimme kaksi vetysidottua kompleksia. Pysyvin rakenne syntyy hiilimonoksidin sitoutuessa hiilestä vetyperoksidin OH-ryhmään ja laskettu interaktioenergia molekyylien välillä on* $-9.0\ kJ\,mol^{-1}$ *CCSD(T)/6-311++G(3df,3pd)//MP2/6-311++G(3df,3pd) -laskutasolla. Hapesta sitoutunut vetysidottu kompleksi on lähes puolet heikompi kuin hiilestä sitoutunut kompleksi. Kokeellisesti me havaitsimme ainoastaan alhaisimman energian muodon,* H_2O_2-CO*:n, Ar, Kr ja Xe-matriiseissa. Vetysidos muuttaa molekyylien värähdysspektrejä, ja näiden siirtymien avulla erotamme kompleksin värähdykset monomeereista. Kompleksin fotolysointi ultraviolettivalolla hajottaa kompleksin ja tuottaa pääasiassa veden ja hiilidioksidin välisen vetysidotun kompleksin. Havaitsimme myös hieman HCO ja trans-HOCO radikaaleja fotolyysin ja sitä seuranneen lämmityksen jälkeen.*

6-311++G(2d,2p) basis set at both MP2 and MP3 levels, no difference between the bond distances of the hydrogen bonded and the non-bonded O-H can be found. At the MP2/6-311++G(3df,3pd) level, a difference of 0.01 Å is noted. The calculated intermolecular distances for the oxygen-attached complex are slightly longer than for the carbon-attached complex, which indicates a weaker interaction between the complexed subunits. It can also be noted that the hydrogen bonds in both the HOOH – CO and HOOH – OC complexes are tilted from linearity by an angle of approximately 10°.

Energetics: The BSSE-corrected interaction energies of the H_2O_2 – CO complexes are shown in Table 2. It is evident that the carbon-attached HOOH – CO complex has a stronger bond than the oxygen-attached HOOH – OC complex. At the MP2/6-311++G(2d,2p) level, the interaction energies are -9.4 and -3.2 kJ mol^{-1}, respectively, for these two complexes. Increasing the basis set by adding polarization functions increases the interaction by ~ 0.5 kJ mol^{-1}. The CCSD(T) level of theory is regarded as a reliable approach for the estimation of interaction energies for weak interactions,[23] and this level has been used for these complexes with the use of the equilibrium structures calculated at the MP2 or MP3 levels. It is interesting that the CCSD(T) calculations give a weaker interaction for the carbon-attached complex, but a stronger interaction for the oxygen-attached complex. For both complexes, the change upon introducing the CCSD(T) level is approximately 1 kJ mol^{-1}, which is approximately 10 % of the total interaction energy for HOOH – CO and 25 % for HOOH – OC. This behavior can be compared with the H_2O – CO complex in which extensive energy decomposition analysis indicates that, for the carbon-attached complex, the main interaction energy contribution comes from first-order electrostatic interactions.[24, 25] For the H_2O – OC complex, the dispersion energy plays a much larger role in the interaction than for the carbon-attached complex, and an increase of the interaction energy was observed from the MP2 to the CCSD(T) level,[26] similar to that of the HOOH – OC complex in this study. Additionally, the hydrogen-bonded complexes that involve H_2O_2 have a stronger bond to CO than the corresponding water complexes, which indicates that hydrogen peroxide acts as a stronger hydrogen bond donor than water. When comparing the isoelectronic molecules CO and N_2, it is noted that the nitrogen molecule forms a stronger bond with H_2O_2 than that of the oxygen-attached HOOH – OC complex, but it has a weaker bond compared with that of the HOOH – CO complex. The calculated HOOH $\cdots$ N_2 interaction energy at the MP2/6-31++G(2d,2p) level is -6.0 kJ mol^{-1}.[13]

Table 2. The BSSE-corrected interaction energies (in kJ mol^{-1}) of the H_2O_2 – CO complexes.

	MP2/ 6-311++G(2d,2p)	MP3/ 6-311++G(2d,2p)	MP2/ 6-311++G(3df,3pd)
HOOH – CO			
MP2	– 9.444	–	– 10.110
MP3	– 7.391	– 8.101	– 8.044
MP4D	– 7.571	– 8.238	– 8.246
MP4DQ	– 6.987	– 7.728	– 7.541
MP4SDQ	– 7.705	– 8.335	– 8.242
CCSD	– 7.059	– 7.797	– 7.592
CCSD(T)	– 8.334	– 8.915	– 9.040
HOOH – OC			
MP2	– 3.165	–	– 3.849
MP3	– 6.303	– 3.576	– 4.371
MP4D	– 3.431	– 3.348	– 4.125
MP4DQ	– 3.343	– 3.266	– 3.987
MP4SDQ	– 3.409	– 3.328	– 4.069
CCSD	– 3.586	– 3.498	– 4.242
CCSD(T)	– 3.926	– 3.809	– 4.742

Vibrational properties: The calculated intra- and intermolecular vibrational frequencies, IR intensities and vibrational shifts upon complexation for HOOH – CO and HOOH – OC are presented in Table 3 and Table 4, respectively. In hydrogen-bonded complexes, the stretching frequencies of the proton donor associated with the hydrogen bond, in this case the O–H bond of hydrogen peroxide, typically undergoes a red-shift to lower frequencies compared with those of the monomer.[27] For HOOH – CO, the OH stretching frequency upon complexation is expected to shift by -54 cm^{-1} compared with the monomer value. The MP2/6-311++G(2d,2p) calculation predicts only a small upward shift of approxi-

Table 3. The calculated harmonic vibrational frequencies, vibrational shifts upon complexation and IR intensities of the HOOH – CO complex at various levels of theory.

	MP2/6-311++G(2d,2p)			MP3/6-311++G(2d,2p)			MP2/6-311++G(3df,3pd)		
ν OH	3830.9	+ 1.6	41	3916.4	+ 2.7	36	3853.0	+ 0.6	38
ν OH_{HB}	3775.5	– 53.7	259	3885.1	– 26.9	206	3786.8	– 65.1	265
ν C≡O	2136.5	+ 16.7	30	2322.1	+ 20.2	88	2157.0	+ 16.9	30
δ OOH	1476.9	+ 29.5	3	1519.7	+ 24.4	3	1470.6	+ 35.3	5
δ OOH	1354.8	+ 18.0	89	1400.9	+ 14.3	86	1352.1	+ 18.3	87
ν OO	913.4	+ 0.5	1	981.9	+ 1.0	1	978.5	– 0.1	1
τ HOOH	547.5	+ 149.5	121	525.1	+ 112.4	128	560.9	+ 150.8	104
	238.7		97	226.4		94	248.9		98
Inter-	153.2		< 1	145.6		< 1	158.8		< 1
molecular	127.6		1	120.5		1	131.7		1
modes	86.2		7	81.4		11	87.9		7
	31.5		< 1	27.5		1	31.8		< 1
ZPVE[a]	87.76			90.63			88.39		

[a] Zero-point vibrational energy in the units of kJ mol^{-1}.

0947-6539/01/0708-1672 $ 17.50+.50/0 *Chem. Eur. J.* **2001**, *7*, No. 8

Table 4. The calculated harmonic vibrational frequencies, vibrational shifts upon complexation and IR intensities of the HOOH–OC complex at various levels of theory.

	MP2/6-311++G(2d,2p)			MP3/6-311++G(2d,2p)			MP2/6-311++G(3df,3pd)		
	ω [cm^{-1}]	$\Delta\omega$ [cm^{-1}]	I [$km\,mol^{-1}$]	ω [cm^{-1}]	$\Delta\omega$ [cm^{-1}]	I [$km\,mol^{-1}$]	ω [cm^{-1}]	$\Delta\omega$ [cm^{-1}]	I [$km\,mol^{-1}$]
ν OH	3840.1	+10.8	121	3928.1	+14.4	115	3865.7	+13.3	126
ν OH_{HB}	3829.0	−0.2	48	3913.4	+1.4	52	3851.5	−0.4	45
ν C≡O	2118.3	−1.5	52	2295.0	−6.9	121	2138.2	−1.9	54
δ OOH	1456.5	+9.1	2	1505.8	+10.5	1	1446.7	+11.4	2
δ OOH	1343.8	+7.0	105	1394.4	+7.8	97	1340.2	+6.4	102
ν OO	914.3	+1.4	1	981.6	+0.7	1	940.3	+1.7	1
τ HOOH	444.8	+46.8	166	459.5	+46.8	164	462.1	+52.0	144
	163.1		77	165.0		85	187.1		84
Inter-	102.7		1	102.7		1	111.6		1
molecular	73.7		<1	68.8		<1	74.3		<1
modes	51.6		9	47.7		7	54.7		7
	22.4		1	14.9		1	22.3		1
ZPVE[a]	85.89			88.98			86.70		

[a] Zero-point vibrational energy in the units of $kJ\,mol^{-1}$.

mately 2 cm^{-1} of the noncomplexed OH bond of H_2O_2. Simultaneously, the OH bond that forms the hydrogen bond with CO becomes stronger, whereas the unperturbed OH bond of the monomer appears much weaker. This is in agreement with general trends observed for proton donors that are involved in hydrogen-bonded complexation.[27] For the HOOH–CO complex, CO is a proton acceptor and the C≡O bond becomes stronger, as evidenced by the blue-shift of the vibrational wavenumber. The opposite effect is noted for the OH vibrational band of the oxygen-attached HOOH–OC complex, for which the wavenumber increases compared with the monomer value. This behavior is due to the interaction with the slightly more positively-charged oxygen of CO. The O–H bond of H_2O_2 is contracted. Simultaneously, the C≡O bond becomes weaker and the vibrational wavenumber undergoes a red-shift. The opposite behaviour of these vibrational modes in the oxygen- and carbon-attached complexes can easily be used as a structural fingerprint for each species. This approach has been employed in the case of H_2O–CO[25, 26] and HF–CO complexes[28] to distinguish the two different forms of the complexes, that is, the carbon-attached and the oxygen-attached species.

The OOH bending modes of H_2O_2 shifts to higher wavenumbers for both complex structures. The H_2O_2 bending is already quite strong in the monomer, and its shift upon complexation can be used as an additional fingerprint for the HOOH–CO/OC complexes. For the carbon-attached complex, it is shifted by +18 cm^{-1} (MP2) from the monomer value. For the oxygen-attached complex, the shift is about half of this at all levels. The O–O stretching mode is insensitive towards complexation and cannot be used for experimental identification of the complexes.

The shifts of the vibrational absorptions of proton-donor and -acceptor stretching vibrations are sensitive to the geometry of the complex. The most rigorous studies of monomeric H_2O_2 indicate that the CCSD(T)/cc-PVQZ level is needed in order to achieve relatively good structural parameters.[29, 30] This computational level is too expensive for hydrogen-bonded complexes, however. Instead, the MP2 calculations used in this study are a good compromise between accuracy and computational cost. Still, these calculations tend to overestimate the vibrational shifts induced by complexation, and therefore, reference calculations at the MP3 level are included in this study as well. The MP3 calculations were previously shown to correct the overestimated harmonic MP2-shifts, and better reproduce the vibrational shifts in $(HF)_2$ and $(H_2O)_2$.[31, 32] For the HOOH–CO complex, the MP3 calculations reduce the predicted vibrational shifts of the complexed OH bond and the torsional mode. The shift of the hydrogen-bonded OH changes from −54 to −27 cm^{-1} and the shift of the torsional mode is +112 cm^{-1} at the MP3 level. For the oxygen-attached HOOH–OC complex, the vibrational shifts of the hydrogen peroxide vibrational modes are mainly unaffected by the increase of electron correlation. For both complex forms, a notable effect is found for the CO stretching mode. For HOOH–CO, it is shifted by +20 cm^{-1} at the MP3 level compared with the monomer wavenumber, whereas the shift is +16 cm^{-1} at the MP2 level. For the HOOH–OC complex, the CO stretching mode shifts by approximately −7 cm^{-1} compared with the monomer value, while the MP2 calculations shifts only by −2 cm^{-1}.

Experimental results

The observed HOOH–CO complex bands and their shifts are presented in Table 5, and they are compared with the monomer vibration bands in Ar, Kr and Xe matrices.

Argon matrix: Figure 2 shows the OH stretching region of the IR absorption spectrum of H_2O_2 in solid Ar when the concentration of CO is increased. The top trace was obtained for a sample that contains only hydrogen peroxide and no CO, and the doublet of the OH stretching mode of H_2O_2 is clearly visible as was reported earlier.[15] With an increase in the amount of CO in the sample, a new band grows at approximately 3548 cm^{-1}. This band is shifted by −40 cm^{-1} compared with the monomer band, and is between the calculated shifts of −54 and −27 cm^{-1} at the MP2 and MP3 levels of theory for the lower-energy (carbon-attached) form,

Table 5. Experimentally observed vibrational bands (in cm^{-1}) of HOOH – CO and their comparison with the monomer bands.

	Monomers[a]			HOOH – CO					
	Ar	Kr	Xe	ν(Ar)	$\Delta\nu$(Ar)	ν(Kr)	$\Delta\nu$(Kr)	ν(Xe)	$\Delta\nu$(Xe)
ν_5, ν_1 (OH str.)	3597.0	3583.6	3568.0						
ν_5, ν_1 (OH str.)	3587.8	3574.0	3560.0	3547.7	−40.1	3545	−29.0	3543.1	−16.9
$\nu_2+\nu_6$	2649.7	2649.7	2639.6						
$\nu_2+\nu_6$	2636.3	2636.3	2628.5	(2671)		(2664)			
C≡O str.	2138.6	2135.7	2133.2	2153.1	+14.5	2150.7	+15.0	2146.9	+13.7
ν_2 (OOH bend)	1372.7	1376.0	1369.3	(1396.7)	(+24.0)	1395.2	+19.2		
	1365.4	1367.6	1362.8						
ν_6 (OOH bend)	1277.0	1273.7	1270.3	1286.8	+9.8	1283.9	+10.2	1279	+8.7
	1270.9	1268.7	1265.7						
ν_3 (O–O str.)	869[b]			(869.5)	(+0.5)				
ν_4 (torsion)	373[c]								

[a] From ref. [15]. [b] Raman measurements from ref. [50]. [c] From ref. [33].

HOOH – CO. Experiments performed with a CO:Ar ratio of 100:1 [trace d) in Figure 2] indicates that most of the deposited hydrogen peroxide is in a complexed form, and two OH stretching bands are seen: the hydrogen bonded OH stretch shifted to lower wavenumbers and the non-bonded OH stretch at the same position as the monomer band.

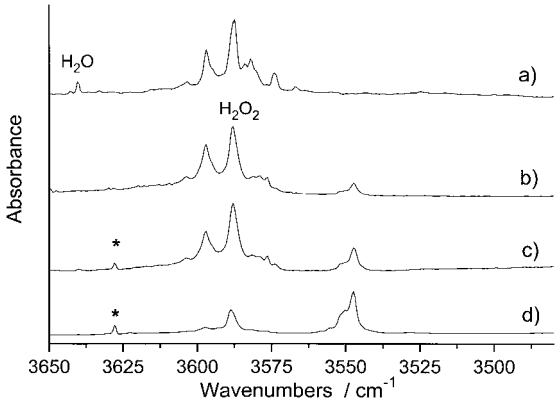

Figure 2. The OH stretching region of H_2O_2 in the HOOH – CO complex upon double-doping experiments of CO/H_2O_2/Ar at different amounts of CO mixed into the matrix: a) no CO, b) Ar:CO = 1:1000, c) Ar:CO = 1:500, d) Ar:CO = 1:100. The band marked with an asterisk is due to water impurity.

Another strong band of monomeric hydrogen peroxide is the OOH antisymmetric bending mode, observed as a doublet at 1273 and 1265 cm^{-1}.[15] When the CO concentration in the samples was increased, a new band was found at 1287 cm^{-1}, between the bands of the monomer and the dimer (1293.2 cm^{-1})[15] absorptions. The band shows a blue-shift of 14 – 22 cm^{-1}, and agrees well with the computational estimates of a shift of +18 and +14 cm^{-1} at the MP2 and MP3 levels, respectively. Other weaker bands at 2671 and 1397 cm^{-1} can be assigned to the HOOH – CO complex since these bands can be easily related to the monomer bands previously observed. The observed bands are assigned as $\nu_2+\nu_6$ and ν_2 of H_2O_2, which is complexed with CO. The O–O stretching mode of H_2O_2 is known to be very weak and it has been observed only for some dimeric or multimeric H_2O_2 species in low temperature argon matrices at 869/866 cm^{-1}.[15] Upon complexation with carbon monoxide, a weak signal appears at 869.5 cm^{-1}, which can be tentatively assigned to the O–O stretching of the HOOH – CO complex. The computations also indicate that this mode is quite weak and only nominally shifted from the position of the monomer band. The harmonic vibrational calculations predict a large blue-shift of the torsional mode from that of the monomer (373 cm^{-1})[33], but this shift is most likely overestimated and could not be reproduced experimentally.

The most conclusive evidence for the carbon-attached HOOH – CO complex is found in the C≡O stretching region. Increasing the amount of CO in the sample leads to a new absorption at 2153 cm^{-1}. This band has a higher wavenumber than that of the corresponding water complex (2149 cm^{-1}),[26, 34] and we assign it to the carbon-attached complex HOOH – CO. No clear indications of the higher-energy form HOOH – OC were found based on the theoretically-predicted downward shift of the C≡O absorption. This behavior can be connected to the method of preparing the complex in the matrix. The complex subunits are mixed in the gas phase and then sprayed onto the cold surface. In the gas phase, the thermal energy is sufficient to overcome the energy barrier separating the two local minima structures of the H_2O_2 – CO complex. Thus, the higher-energy form relaxes (probably on the matrix surface) to the lower-energy, carbon-attached form, which is isolated in the matrix. A similar behaviour was seen earlier for CO complexes with water[25, 26] and formic acid[35] when only the lower-energy form was observed when the mixtures were deposited out of the gas phase. In Kr and Xe environments, both forms of H_2O – CO were found after photoinduced decomposition of formic acid.[25, 26]

A previous attempt to identify the H_2O_2 – CO complex was performed by Tso and Lee[12] with the use of H_2O/H_2O_2/CO mixtures in solid oxygen. They reported vibrational bands of complexed H_2O_2 at 3542.6 (ν_1) and 1278.2 cm^{-1} (ν_2), and a complexed CO band at 2150.9 cm^{-1}, which were assigned to the HOOH – CO complex. These band positions are in good agreement with our observations. However, the band reported by Tso and Lee at 1267.5 cm^{-1} is not due to the HOOH – CO complex as was originally reported,[12] being most likely due to larger clusters of deposited molecules.

Krypton and xenon matrices: The OH stretching vibration of the HOOH – CO complex is shown in Figure 3 in the Ar, Kr and Xe matrices. The shifts of the vibrational modes of the

0947-6539/01/0708-1674 $ 17.50+.50/0 *Chem. Eur. J.* **2001**, *7*, No. 8

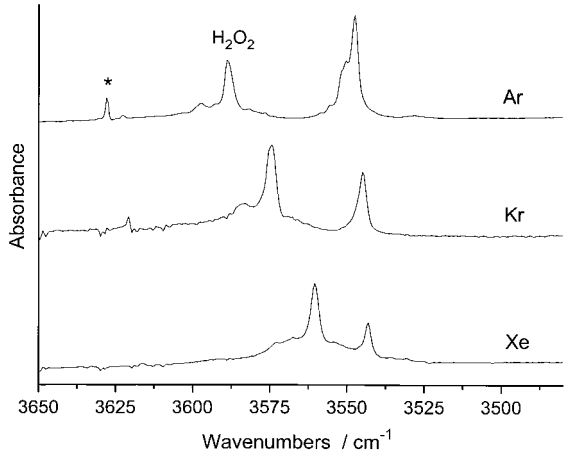

Figure 3. The OH stretching bands of the HOOH – CO complex in Ar, Kr and Xe environments.

H_2O_2 monomer and the H_2O_2 – CO complex are listed in Table 6. It is thus shown that the OH bond that is involved in the interaction is insensitive to the change of the environment. The band of the complexated OH is found at 3548 cm^{-1} in Ar, and it shifts to 3545 and 3543 cm^{-1} in Kr and Xe, respectively.

Table 6. The observed vibrational shifts of the hydrogen-bonded OH stretching mode in the HOOH – CO complex compared with the monomer wavenumbers.

	H_2O_2		H_2O_2 – CO		
	ν [cm^{-1}]	$\Delta\nu_g$[a] [cm^{-1}]	ν [cm^{-1}]	$\Delta\nu_g$[a] [cm^{-1}]	$\Delta\nu_g$[b] [cm^{-1}]
gas phase	3608[c]				
Ar	3587.8[d]	– 20.2	3547.7	– 60.3	– 40.1
Kr	3574.0[d]	– 34.0	3545	– 63.0	– 29.0
Xe	3560.0[d]	– 48.0	3543	– 65.0	– 17.0

[a] Vibrational shift compared with the gas phase wavenumber of H_2O_2 monomer. [b] Vibrational shift compared with the vibrational wavenumber of the monomer in the matrix. [c] From ref. [51]. [d] From ref. [15].

On the other hand, the H_2O_2 monomer is much more sensitive to the change of the environment. It can be reasoned that the complexated OH-tail of H_2O_2 does not interact with surrounding atoms as strongly as the monomer does. This feature indicates that a molecule (H_2O_2) is not simply solvated in the matrix, but it is "complexed" with a rare gas atom, that is specific interactions with some of the cage atoms exist.

In general, an isolated molecule in a low-temperature matrix cage is held by van der Waals interactions, which are essentially different from the directed and stronger hydrogen bonds. However, an interaction between the isolated molecule and the cage atoms exists, and the strength of the interaction is proportional to the proton-acceptor ability of the rare gas atom as well as the steric hindrance.[36, 37] Yukhnevich suggested that instead of comparing the shift of the band of the complex with that of the unperturbed monomer in the matrix, it would be more appropriate to compare the vibrational mode of the complex with that of the monomer in the gas phase, because the matrix value already involves a "complexed" species.[36] This comparison is also included in Table 6. For the HOOH – CO complex, the shifts that are compared with the gas phase values show a very small dependence on the change of the polarisable environment, which demonstrates a small solvation effect on the "complexed" vibrations.

When the CO stretching wavenumber of the CO subunit in the HOOH – CO complex is compared with that of unperturbed CO, very small changes are noted when the matrix is changed from Ar to Xe. In experiments where both subunits are simultaneously deposited from the gas phase, the blue-shifted CO band that belongs to the carbon-attached complex is the only complex band observed in this spectral region, which indicates that the interaction between H_2O_2 and CO is not strong enough to stabilize the HOOH – OC form.

Both the ν_2 and ν_6 OOH bending modes are observed in solid Kr at 1397 and 1284 cm^{-1}, respectively. The ν_2 band of H_2O_2 in Xe was not observed. The ν_6 band of the complex, which is one of the strongest bands of the H_2O_2 monomer, was observed at 1279 cm^{-1} in Xe. It is shifted by a few wavenumbers from its position in the Ar and Kr matrices, similar to the shift observed for the monomer.

UV photolysis of the HOOH – CO complex: Irradiation of the HOOH – CO complex in solid Ar at 266 and 230 nm decomposes the hydrogen peroxide molecule in the complex. Simultaneously with the observed disappearance of the H_2O_2 vibrational absorptions, new absorption bands appear at 3728.0, 2347.0, 2345.1, 666.3 and 655.2 cm^{-1} in Ar matrices. Also, minor traces of *trans*-HOCO are found after photolysis, which are identified mainly by the strong C=O stretching absorption found at 1843.6 cm^{-1} in solid Ar.[38] The new absorption bands observed after photolysis at 3728.0, 2347.0 and 655.2 cm^{-1} can be assigned to the H_2O – CO_2 complex, according to previous work on this complex in solid N_2[39] and O_2.[40] The bands at 2341.1 and 666.3 cm^{-1} belong to monomeric CO_2. All of the new vibrational bands observed after UV photolysis (and annealing) of HOOH – CO are shown in Table 7.

Table 7. Vibrational bands observed after photolysis and annealing of HOOH – CO complex in various rare gas matrices.

Ar	Kr	Xe	
3728.7			H_2O – CO_2
2348.9 (sh)			H_2O – CO_2
2347.0	2344.3	2338.5	H_2O – CO_2
2345.1	2340.6	2334.4	CO_2
2340.2			CO_2
1863.4	1860.0	1856.7	HCO
1843.6	1839.8	1834.4	*trans*-HOCO
666.3	661.8		CO_2
655.2	658.2	657.7	H_2O – CO_2

In an Ar matrix, the kinetic scheme presented in Equation (1) was suggested to describe the UV photolysis of monomeric H_2O_2:[9]

$$H_2O\cdots O(^3P) \rightleftharpoons H_2O_2 \longrightarrow OH+OH \quad (1)$$

Furthermore, no essential losses (leaks) by additional channels, such as shown in Equation (2), were found experimentally.

$$H_2O_2 \rightarrow H_2+O_2 \text{ or } H_2O_2 \longrightarrow H+HO_2 \quad (2)$$

The formation of a $H_2O\cdots O$ van der Waals complex is favored in the photodissociation at approximately 250 nm (83%), whereas the reaction that produces two OH radicals only has a 17% probability. It should be remembered that the cage exit probability of the formed OH radicals is small in solid Ar, and their concomitant reaction produces H_2O and O as previously reported for the gas phase species.[1, 41, 42]

When complexed H_2O_2 decomposes, the amount of CO_2 that is complexed with H_2O increases. A number of possible reaction paths for the formation of CO_2 can be suggested. First, upon photolysis, an excited singlet O atom is formed, which then recombines with CO. However, once the O atom has relaxed to its ground state (^3P), the reaction with CO is spin-forbidden. Another possibility is the formation of a charge-transfer system, such as $(H_2O)^+O^-$, which has been suggested to be involved in the observed UV-induced recombination of the $H_2O\cdots O$ complex into H_2O_2.[9]

A dissociation path that produces OH radicals from monomeric H_2O_2 upon complexation produces a ternary system that is comprised of two OH radicals and a CO molecule. A stepwise reaction that produces first OH and HOCO might then lead in a secondary step to a hydrogen abstraction by the second OH radical to form H_2O+CO_2. A further possibility that leads to a H_2O-CO_2 complex could involve carbonic acid, H_2CO_3, by recombination of HOCO with an OH radical that is also trapped in the same rare gas cage. Carbonic acid, which has the same stoichiometry as the precursor complex in our study, is known to be thermodynamically unstable, and produces water and carbon dioxide when it decomposes.[43] If carbonic acid is produced from hot OH radicals and CO in the same cage, it is probable that it would decompose to its more stable constituents, which are then also trapped in the matrix. These two reaction paths assume that both of the resulting OH radicals stay in the same cage. However, some escape of OH radicals is known to occur under UV photolysis of H_2O_2.[9] In accordance with this observation, the formation of HOCO observed during HOOH–CO photolysis indicates that some OH radicals escape the rare gas cage and the remaining CO and OH radicals recombine to form monomeric HOCO.

A prolonged UV photolysis of the H_2O_2/CO argon matrices leads to an increase of uncomplexed CO_2 that absorbs at 2345.1 cm^{-1} (shoulder at 2340.2 cm^{-1}) and at 666.3 cm^{-1}. These bands are in agreement with the C–O stretching and OCO bending bands of CO_2 reported in the literature.[44] The C–O stretching bands of the CO_2 monomer are found in Figure 4 along with the bands of the complex. The formation of unperturbed CO_2 can be explained by UV-induced photodecomposition of the HOCO molecules that produce CO_2 and H atoms. The threshold for this reaction has previously been reported by Jacox to be near 300 nm.[38]

The photolysed matrix samples were annealed at approximately 25 K, which mobilizes the hydrogen atoms that are produced in the matrix by photolysis of HOCO. This is evidenced mainly by the increase of HCO, which absorbs at 1863.4 cm^{-1} in solid Ar,[45] formed from the reaction between hydrogen atoms and free CO molecules in the matrix. Also, the vibrational bands of HOCO are observed to grow upon annealing. The annealing-induced vibrational bands of HCO and HOCO in the 1800–1900 cm^{-1} region are shown in Figure 5.

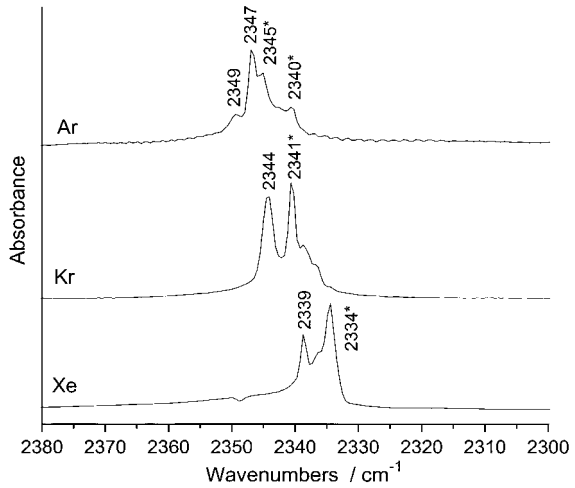

Figure 4. H_2O-CO_2 and CO_2 absorptions in the CO_2 stretching fundamental region in various matrix environments after 300 nm photolysis. Monomeric CO_2 bands are marked with asterisks.

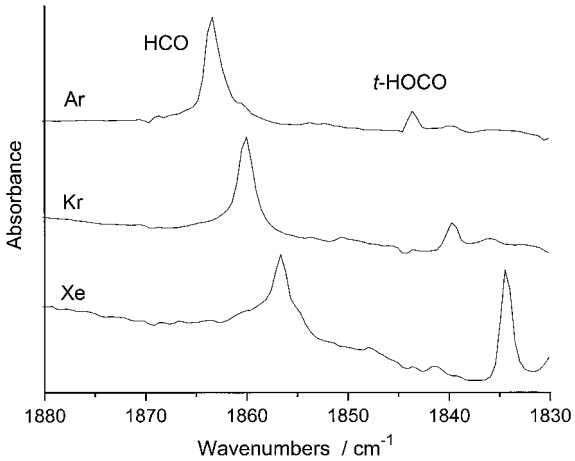

Figure 5. HCO and *trans*-HOCO in Ar, Kr and Xe matrices obtained in annealing at 40 and 45 K, respectively. The H_2O_2/CO/Rg (Rg = Ar, Kr, Xe) matrices were preliminary photolyzed by UV radiation.

The photolysis in solid Kr and Xe produced similar products as those in solid Ar. In solid Kr, the C–O stretching band of CO_2 displays two components at 2344.3 and 2340.6 cm^{-1}, as shown in Figure 4. These components can be assigned to the complexed CO_2 and monomeric CO_2, respectively. In solid Xe, the complexed CO_2 stretching band is found approximately 4 cm^{-1} higher than the absorption of the monomeric CO_2, similar to the bands of the two species in a Kr matrix. The bending mode of CO_2 in the H_2O-CO_2 complex is assigned at 658.2 and 657.7 cm^{-1} in solid Kr and Xe, respectively. No water stretching bands due to a H_2O-CO_2 complex were found in the Kr or Xe matrices. This is probably because these bands are quite weak and they are heavily overlapped by water impurity bands, both monomeric and complexed with various species (O, O_2, N_2, H_2O, CO).

0947-6539/01/0708-1676 $ 17.50+.50/0 *Chem. Eur. J.* **2001**, *7*, No. 8

The HCO absorptions were found in Kr and Xe at 1860.0 and 1856.7 cm^{-1}. The strongest band of *trans*-HOCO observed in solid Ar was identified for the first time in Kr and Xe at 1839.8 and 1834.4 cm^{-1}, respectively. What is interesting in these species is that they appear only after annealing of the photolyzed matrix, whereas in Ar, some HOCO was also produced during photolysis. Moreover, in solid Xe, a larger amount of HOCO than HCO is formed, which reverses the situation compared with the other matrices. This is shown in Figure 5. These observations agree with the reports of H_2O_2 photolysis in Xe matrices[11] for which no OH radicals were formed upon irradiation. Indeed, suppression of the cage exit of OH radicals does not allow monomeric HOCO to be formed in the photolysis of HOOH–CO. On the other hand, the formation of hydrogen atoms occurs in Xe and they become globally mobile upon annealing,[46] as evidenced by the increase of the amounts of HCO and HOCO. Nevertheless, it must be remembered that H atoms can still be generated from the HCO–OH intermediate. Furthermore, the amount of H atoms stabilized in the Xe matrix after photolysis is minor because practically no HXeH[47] appears during annealing.

Conclusion

We have studied complexes between hydrogen peroxide and carbon monoxide with the use of experimental matrix isolation techniques and ab initio calculations. Computationally, two stable configurations for the complex were found and they both show an almost linear hydrogen bond from the OH tail of H_2O_2. The lower-energy form, a carbon-attached H_2O_2–CO complex, has an interaction energy of $-9.0\ kJ\,mol^{-1}$ at the CCSD(T)/6-311++G(3df,3pd)//MP2/6-311++G(3df,3pd) level. The interaction energy obtained for the higher-energy form, where CO is attached to the oxygen end (HOOH–OC), is $-4.7\ kJ\,mol^{-1}$ at the same level of theory. Only the HOOH–CO complex was found experimentally in low temperature matrices. Upon UV photolysis of the matrix samples, the vibrational absorptions of HOOH–CO decrease, in correlation with the increase of vibrational bands of the H_2O–CO_2 complex. Simultaneously, a minor amount of HCO and *trans*-HOCO is found after photolysis in solid Ar. In the Kr and Xe matrices, traces of HCO and HOCO are noted only after subsequent annealing, which mobilizes hydrogen atoms in the matrices.

Experimental and Computational Section

The preparation of hydrogen peroxide matrices is thoroughly described in ref. [15]. Briefly, the hydrogen peroxide was deposited by flushing urea hydrogen peroxide (UHP, Aldrich, 98% purity) at room temperature with the matrix gas (Ar, Kr or Xe) that contains different amounts of CO. The absolute concentration of hydrogen peroxide could not be determined, but its relative concentration was varied by changing the deposition rate and/or deposition temperature. The rare gas/CO ratio ranged from 1:100 to 1:1500. The gas mixture was deposited onto substrates (CsI) in closed cycle helium cryostats (Air Products, DE 202A and HS-4) at temperatures of 7.5 and 15 K, respectively. The temperature was measured with a silicon diode (accuracy 0.5 K), and a resistive heater provided higher temperatures. The IR absorption spectra of the samples were recorded on a Nicolet 60 SX FTIR-spectrometer (resolution 1.0 cm^{-1}) in the spectral region 400–4000 cm^{-1}. In photolysis, an optical parametric oscillator (OPO Sunlite with FX-1, Continuum) was used to deliver UV radiation of typical pulse energies of 10 mJ, with a repetition rate of 10 Hz and pulse duration of 5–10 ns.

All calculations were performed with the use of the Gaussian 98 package of computer codes.[48] The applied basis set was the split-valence, 6-311G-type Gaussian functions added with multiple sets of polarizations and diffuse functions to give the 6-311++G(2d,2p) and 6-311++G(3df,3pd) basis sets. The complex properties were considered by the supermolecular Møller–Plesset perturbation theory to the second (MP2) and third (MP3) order. The interaction energy was estimated as the difference of the total energy between the complex and the monomers at infinite distance, where the monomer wavefunctions were derived in the dimer centered basis set (DCBS). This approach corresponds to the counterpoise correction proposed by Boys and Bernardi,[49] aimed at the minimization of the basis set superposition error (BSSE) in the interaction energy. The optimized equilibrium structures of the complexes were used to evaluate the interactions energy at higher correlated levels that range from the higher order perturbation theory (MP3, MP4) to the coupled cluster approach (CCSD and CCSD(T)).

Acknowledgement

The authors thank the Academy of Finland for financial support and the CSC-Center for Scientific Computing Ltd. (Espoo, Finland) for computational allocation on the SGI Origin 2000 computer.

[1] R. P. Wayne, *Chemistry of Atmospheres*, 2nd ed., Clarendon Press, Oxford, **1991**, Chapter 5.
[2] W. Tsang, R. F. Hampson, *J. Phys. Chem. Ref. Data* **1986**, *15*, 1087.
[3] K. B. Beckman, B. N. Ames, *Physiol. Rev.* **1998**, *78*, 547.
[4] R. F. Carlson, M. S. Anderson, R. E. Johnson, W. D. Smythe, A. R. Hendrix, C. A. Barth, L. A. Soderblom, G. B. Hansen, T. B. McCord, J. B. Dalton, R. N. Clark, J. H. Shirley, A. C. Ocampo, D. L. Matson, *Science* **1999**, *283*, 2062.
[5] D. Fulle, H. F. Hamann, H. Hippler, J. Troe, *J. Chem. Phys.* **1996**, *105*, 1001, and references therein.
[6] *Molecular Complexes in Earth's*, *Planetary*, *Cometary and Interstellar Atmospheres* (Eds.: A. A. Vigasin, Z. Slanina), World Scientific, Singapore, **1998**.
[7] M. L. Salby, *International Geophysics Series*, *Vol. 61*, Academic Press, San Diego, **1996**.
[8] I. M. Svishchev, R. J. Boyd, *J. Phys. Chem. A* **1998**, *102*, 7294.
[9] L. Khriachtchev, M. Pettersson, S. Tuominen, M. Räsänen, *J. Chem. Phys.* **1997**, *107*, 7252.
[10] S. Pehkonen, M. Pettersson, J. Lundell, L. Khriachtchev, M. Räsänen, *J. Phys. Chem. A* **1998**, *102*, 7643.
[11] L. Khriachtchev, M. Pettersson, S. Jolkkonen, S. Pehkonen, M. Räsänen, *J. Chem. Phys.* **2000**, *112*, 2187.
[12] T.-L. Tso, E. K. C. Lee, *J. Phys. Chem.* **1985**, *89*, 1612.
[13] J. Lundell, S. Pehkonen, M. Pettersson, M. Räsänen, *Chem. Phys. Lett.* **1998**, *286*, 382.
[14] J. Goebel, B. S. Ault, J. E. Del Bene, *J. Phys. Chem. A* **2000**, *104*, 2033.
[15] M. Pettersson, S. Tuominen, M. Räsänen, *J. Phys. Chem. A* **1997**, *101*, 1166.
[16] J. A. Dobado, J. Molina, *J. Phys. Chem.* **1993**, *97*, 7499.
[17] O. Mo, M. Yanez, I. Rozas, J. Elguero, *J. Chem. Phys.* **1994**, *100*, 2871.
[18] L. Gonzalez, O. Mo, M. Yanez, *J. Comput. Chem.* **1997**, *18*, 1124.
[19] J. A. Dobado, J. Molina, *J. Phys. Chem.* **1994**, *98*, 1819.
[20] O. Mo, M. Yanez, I. Rozas, J. Elguero, *Chem. Phys. Lett.* **1994**, *219*, 45.
[21] J. A. Dobado, J. Molina, *J. Phys. Chem.* **1994**, *98*, 7819.
[22] J. A. Dobado, J. Molina, *J. Phys. Chem. A* **1999**, *103*, 4755, and references therein.
[23] G. Chalasinski, M. M. Szczesniak, *Chem. Rev.* **1994**, *94*, 1723.
[24] J. Lundell, *J. Phys. Chem.* **1995**, *99*, 14290.
[25] J. Lundell, Ph. D. Dissertation, University of Helsinki, *1995*.
[26] J. Lundell, M. Räsänen, *J. Phys. Chem.* **1995**, *99*, 14301.

[27] G. C. Pimentel, A. L. McLellan, *The Hydrogen Bond*, Freeman, San Francisco, **1960**.
[28] G. Schatte, H. Willner, D. Hoge, E. Knözinger, O. Schrems, *J. Phys. Chem.* **1989**, *93*, 6025.
[29] J. Koput, *Chem. Phys. Lett.* **1995**, *236*, 516.
[30] T. Helgaker, J. Gauss, P. Jørgensen, J. Olsen, *J. Chem. Phys.* **1997**, *106*, 6430.
[31] J. G. C. M. van Duijneveldt-van de Ridjt, F. B. van Duijneveldt, *J. Comput. Chem.* **1992**, *12*, 399.
[32] B. Silvi, R. Wieczorek, Z. Latajka, M. E. Alikhani, A. Dkhissi, Y. Bouteiller, *J. Chem. Phys.* **1999**, *111*, 6671.
[33] J. A. Lannon, F. D. Verderame, R. W. Anderson Jr., *J. Chem. Phys.* **1971**, *54*, 2212.
[34] H. Dubost, *Chem. Phys.* **1976**, *12*, 139.
[35] J. Lundell, M. Räsänen, *J. Phys. Chem.* **1993**, *97*, 9657.
[36] M. O. Bulanin, V. P. Bulychev, K. G. Tokhadze, *J. Mol. Struct.* **1989**, *200*, 33.
[37] G. V. Yukhnevich, *Spectrosc. Lett.* **1997**, *30*, 901.
[38] M. E. Jacox, *J. Chem. Phys.* **1988**, *88*, 4598.
[39] L. Fredin, B. Nelander, G. Ribbegård, *Chem. Scripta* **1975**, *7*, 11.
[40] T.-L. Tso, E. K. C. Lee, *J. Chem. Phys.* **1985**, *89*, 1618.
[41] J. Lelieved, P. J. Crutzen, *Nature* **1990**, *343*, 227.
[42] D. W. Gunz, M. R. Hoffman, *Atmos. Environ.* **1990**, *24A*, 1601.
[43] M. T. Nguyen, G. Raspoet, L. G. Vanquickenborne, P. T. van Duijnen, *J. Phys. Chem. A* **1997**, *101*, 7379.
[44] M. J. Irvine, J. G. Mathieson, A. D. E. Pullin, *Aust. J. Chem.* **1982**, *35*, 1971.
[45] D. E. Milligan, M. E. Jacox, *J. Chem. Phys.* **1969**, *51*, 277.
[46] J. Eberlein, M. Creuzburg, *J. Chem. Phys.* **1997**, *280*, 2188, and references therein.
[47] M. Pettersson, J. Lundell, M. Räsänen, *J. Chem. Phys.* **1995**, *103*, 205.
[48] *Gaussian 98*, Revision A.3, Gaussian, Inc., Pittsburgh PA, **1998**.
[49] S. F. Boys, F. Bernardi, *Mol. Phys.* **1970**, *19*, 553.
[50] P. A. Giguere, T. K. K.Srinivasan, *Chem. Phys. Lett.* **1975**, *33*, 479.
[51] M. W. Chase, J. L. Curnutt, A. T. Hu, H. Prophet, A. N. Syverud, L. C. Walker, *J. Phys. Chem. Ref. Data* **1974**, *3*, 311.

Received: September 21, 2000 [F2745]

0947-6539/01/0708-1678 $ 17.50+.50/0